

# Stability of Strange Stars (SS) under Radial Oscillation.

M. Sinha

Dept. of Physics, Presidency College, 86/1 College Street, Kolkata 700 073, India, CSIR-NET fellow, Govt. of India.

J. Dey

UGC Research Professor, Dept. of Physics, Maulana Azad College, 8 Rafi Ahmed Kidwai Road, Kolkata 700 013, India.

M. Dey

Dept. of Physics, Presidency College, 86/1 College Street, Kolkata 700 073, India.

S. Ray

Inter University Centre for Astronomy and Astrophysics, Post Bag 4, Ganeshkhind, Pune 411007, India.

S. Bhowmick

Department of Physics, Barasat Govt. College, Barasat, North 24 Parganas, W. Bengal, India.

A realistic Equation of State (EOS) leads to strange stars (ReSS) which are compact in the mass radius plot, close to the Schwarzschild limiting line [1]. We carry out a stability analysis under radial oscillations and compare with the EOS of other SS models. We find that the ReSS is stable and an M-R region can be identified to that effect.

## 1. Introduction

The radial mode oscillation, being the simplest mode of neutron star has been considered first to be investigated more than 35 years ago [2]. It can give information about stability of the stellar object under consideration.

The radial modes of neutron star have been studied thoroughly by many authors for cold nuclear matter EOS [3–7]. With this radial modes have been investigated for other type of star, namely Strange Star [8] protoneutron star [9], Hybrid Star [10].

We here present our analysis of radial mode oscillation for Realistic Strange Star (ReSS) Equation of State (EOS).

## 2. Radial oscillations of a relativistic star

Thirty five years ago Chandrasekhar [2] investigated these radial modes. Following him we investigate the same for ReSS.

The spherically symmetric metric is given by the line element

$$ds^2 = -e^{2\nu} dt^2 + e^{2\mu} dr^2 + r^2(d\theta^2 + \sin^2\theta d\phi^2). \quad (1)$$

Together with the energy-momentum tensor for a perfect fluid, Einstein's field equations yield the Tolman-Oppenheimer-Volkoff (TOV) equations which can be solved if we have an EOS,  $p(n_B)$  and  $\epsilon(n_B)$ . Given the central density  $\epsilon_c$ , we can arrive at an  $M - R$  curve by solving the TOV. Without disturbing the spherical symmetry of the background we define  $\delta r(r, t)$ , a time dependent radial displacement of

a fluid element located at the position  $r$  in the unperturbed model which assumes a harmonic time dependence, as

$$\delta r(r, t) = u_n(r) e^{i\omega_n t}. \quad (2)$$

The dynamical equation governing the stellar pulsation in its  $n$ th normal mode ( $n = 0$ , is the fundamental mode) has the Sturm-Liouville's form (for details, see [11]).

$$P(r) \frac{d^2 u_n(r)}{dr^2} + \frac{dP}{dr} \frac{du_n}{dr} + [Q(r) + \omega_n^2 W(r)] u_n(r) = 0, \quad (3)$$

where  $u_n(r)$  and  $\omega_n$  are the amplitude and frequency of the  $n$ th normal mode, respectively. The functions  $P(r)$ ,  $Q(r)$  and  $W(r)$  are expressed in terms of the equilibrium configuration of the star and are given by

$$P(r) = \frac{\Gamma p}{r^2} e^{\mu+3\nu} \quad (4)$$

$$Q(r) = e^{\mu+3\nu} \left[ \frac{(p')^2}{r^2(\epsilon+p)} - \frac{4p'}{r^3} - \frac{8\pi}{r^2}(\epsilon+p) p e^{2\mu} \right] \quad (5)$$

$$W = \frac{(\epsilon+p)}{r^2} e^{3\mu+\nu}, \quad (6)$$

where the varying adiabatic index  $\Gamma$  is given by

$$\Gamma = \frac{(\epsilon+p)}{p} \frac{dp}{d\epsilon}, \quad (7)$$

$\epsilon$  and  $p$  being the energy density and pressure of the unperturbed model, respectively. Eigenfrequencies can be obtained with the boundary conditions,

1. at the centre  $r = 0$ ,  $\delta r = 0$  and
2. at the surface  $\delta p = 0$  leading to  $\Gamma p u(r)' = 0$ ,

Since  $\omega$  is real for  $\omega^2 > 0$ , the solution is oscillatory. However for  $\omega^2 < 0$ , the angular frequency  $\omega$  is imaginary, which corresponds to an exponentially growing solution. This means that for negative values of  $\omega^2$  the radial oscillations are unstable. For a compact star the fundamental mode  $\omega_0$  becomes imaginary at some central density  $\epsilon_c$  less than the critical density  $\epsilon_{critical}$  for which the total mass  $M$  is a maximum. At  $\epsilon_c = \epsilon_c^0$ ,  $\omega_0$  vanishes. All higher modes are zero at even higher central densities. Therefore, the star is unstable for central densities greater than  $\epsilon_c^0$ . To illustrate, we plot the eigen frequencies  $\omega_n$  against  $\epsilon_c$ , the central density in Fig. 1. The fundamental frequency  $\omega_0$  does vanish at some  $\epsilon_c^0$  while the higher modes remain nonzero.

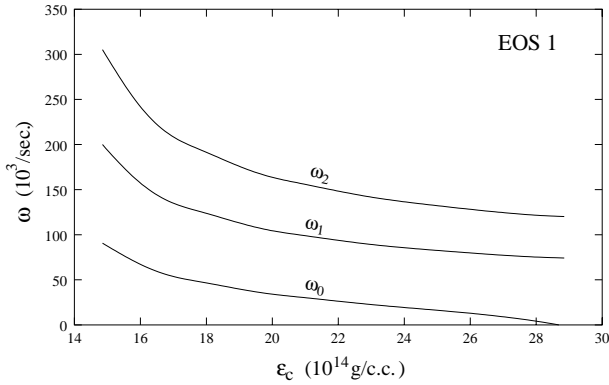


Figure 1: Angular frequency of three different modes against central density for SS1.

Numerical values of masses, radii, central densities and the corresponding eigen frequencies  $\omega_0$ ,  $\omega_1$  and  $\omega_2$  are given in Tables I and II for EOS1 and EOS3 respectively (SS1 and SS2 of Dey et al. 1998). Tables III and IV are for the bag model EOS with different parameters.

### 3. Discussions and summary

ReSS are stable against radial oscillations close to the maximum attainable mass. For example, the EOS of SS1 sustains gravitationally,  $M_{max} \sim 1.4M_\odot$ ,  $R=7$  km with a central number density  $n_c \sim 16n_0$ . However, the fundamental frequency of radial oscillations becomes zero at around  $n_c 9.5 \sim n_0$ , destabilizing the star after  $M=1.36 M_\odot$  with  $R= 7.24$  km (Table I). It is still on the  $\frac{dM}{dR} > 0$  region. Thus the maximum mass star which is stable against radial oscillations has a number density  $\sim 9.5n_0$  at the centre and  $\sim 4.7n_0$  at the surface. Macroscopically, upto this density small vibrations may be sustained.

### References

- [1] M. Dey, I. Bombaci, J. Dey, S. Ray & B. C. Samanta, Phys. Lett. B438 (1998) 123 ; Addendum B447 (1999) 352; Erratum B467 (1999) 303; Indian J. Phys. 73B (1999) 377.
- [2] S. Chandrasekhar, Phys. Rev. Lett. **12** 114 (1964) ; Ap. J, **217** 417 (1964).
- [3] B. K. Harrison, K. S. Thorne, M. Wakano and J. A. Wheeler, "Gravitational Theory and Gravitational Collapse", 1965, (Chicago University of Chicago press).
- [4] G. Channugam, Astrophys. J. **217**, 799 (1977).
- [5] E. N. Glass and L. Lindblom, Astrophys. J. **53**, 93 (1983).
- [6] H. M. V  th and G. Channugam, Astron. and Astrophys. **260**, 250 (1992).
- [7] K. D. Kokkotas and J. Ruoff, Astron. and Astrophys. **366**, 565 (2001).
- [8] O.G. Benvenuto and J.E. Horvath J. E., Mon. Not. of Roy. Astron. Soc. **250**, 679 (1991).
- [9] D. Gondek-Rosi  nska, P. Haensel and J. L. Zdunik, Astron. and Astrophys. **325**, 217 (1997).
- [10] V.K. Gupta, V. Tuli and A. Goyal, Astrophys. J. **579**, 374 (2002).
- [11] C.W. Misner, K.S. Throne and J. A. Wheeler, *Gravitation*, W. H. Free man & Co. New York (1973).

Table I Data for EOS1 (SS1)

$\rho_c 10^{14}$ g/c.c.	$n_c/n_0$	$M/M_\odot$	R km	$\omega_0 10^3$ /sec.	$\omega_1 10^3$ /sec.	$\omega_2 10^3$ /sec.
14.85	5.462	0.407	5.262	90.661	199.957	305.202
15.85	5.798	0.502	5.611	79.884	179.851	275.679
16.85	6.122	0.787	5.940	69.870	162.018	249.011
17.85	6.429	0.893	6.643	47.528	125.267	193.718
18.85	6.735	0.991	6.828	40.784	114.643	178.073
19.85	7.036	1.077	6.970	34.751	105.455	165.102
20.85	7.321	1.133	7.050	30.694	99.662	156.925
21.85	7.605	1.182	7.113	26.848	94.509	149.451
22.85	7.886	1.226	7.161	23.077	89.825	142.620
23.85	8.159	1.261	7.193	19.749	86.070	137.200
24.85	8.427	1.288	7.214	16.693	83.005	132.804
25.85	8.692	1.312	7.228	13.435	80.192	128.753
26.85	8.955	1.333	7.236	9.648	77.588	135.005
27.85	9.212	1.349	7.240	4.943	75.483	122.982
28.85	9.466	1.363	7.240	5.899	73.592	119.295
30.85	9.969	1.381	7.235	—	70.168	114.425
35.85	11.176	1.417	7.194	—	64.144	105.945
40.85	12.333	1.433	7.130	—	59.935	100.169
46.85	13.669	1.437	7.055	—	56.349	95.361

Table II Data for EOS3 (SS2)

$\rho_c 10^{14}$ g/c.c.	$n_c/n_0$	$M/M_\odot$	R km	$\omega_0 10^3$ /sec.	$\omega_1 10^3$ /sec.	$\omega_2 10^3$ /sec.
17.17	6.067	0.423	5.070	86.879	195.416	299.090
18.17	6.382	0.539	5.460	74.016	172.966	264.894
19.17	6.695	0.659	5.794	63.013	153.699	236.761
20.17	7.006	0.781	6.078	53.079	136.745	212.463
21.17	7.298	0.855	6.227	47.332	127.643	199.063
22.17	7.588	0.923	6.351	42.074	119.663	186.932
23.17	7.876	0.986	6.453	37.131	112.402	176.070
24.17	8.156	1.036	6.524	33.069	106.694	167.790
25.17	8.428	1.075	6.575	29.646	102.152	161.274
26.17	8.699	1.110	6.615	26.321	98.030	155.270
27.17	8.967	1.142	6.647	22.992	94.193	149.689
28.17	9.227	1.167	6.667	20.163	91.206	145.298
29.17	9.485	1.188	6.682	17.335	88.518	141.539
30.17	9.741	1.207	6.693	14.307	86.006	137.932
31.17	9.994	1.224	6.691	10.827	83.642	134.554
32.17	10.242	1.237	6.702	6.982	81.741	131.825
33.17	10.488	1.249	6.703	3.351	79.959	129.293
35.17	10.974	1.270	6.698	—	76.694	124.666
40.17	12.148	1.301	6.650	—	70.680	116.215
45.17	13.278	1.316	6.622	—	66.380	110.292
50.17	14.371	1.323	6.573	—	63.141	105.918
55.17	15.537	1.325	6.518	—	60.616	102.546

Table III Data for bag model with B=60 & ms=150

$\rho_c 10^{14}$ g/c.c.	$n_c/n_0$	$M/M_\odot$	R km	$\omega_0 10^3$ /sec.	$\omega_1 10^3$ /sec.	$\omega_2 10^3$ /sec.
6.20	2.421	0.691	8.549	38.964	92.549	142.426
7.20	2.778	1.019	9.544	27.409	73.557	114.644
8.20	3.122	1.240	10.021	20.733	63.870	100.636
9.20	3.454	1.393	10.263	15.915	57.854	92.024
10.20	3.776	1.501	10.393	11.910	53.693	86.161
11.20	4.089	1.581	10.452	7.900	50.628	81.883
12.20	4.396	1.639	10.469	2.159	48.272	78.626
13.20	4.695	1.683	10.462	6.156	46.395	76.048
15.20	5.277	1.741	10.405	—	43.526	72.203
17.20	5.839	1.775	10.321	—	41.429	69.514
23.70	7.560	1.805	10.012	—	37.316	64.404

Table IV Data for bag model with B=75 & ms=150

$\rho_c 10^{14}$ g/c.c.	$n_c/n_0$	$M/M_\odot$	R km	$\omega_0 10^3$ /sec.	$\omega_1 10^3$ /sec.	$\omega_2 10^3$ /sec.
9.83	3.573	1.072	8.923	24.809	73.494	115.482
10.83	3.892	1.198	9.148	20.030	67.175	106.403
11.83	4.203	1.293	9.281	16.097	62.623	99.944
12.83	4.506	1.366	9.356	12.565	59.194	95.089
13.83	4.804	1.422	9.396	9.063	56.480	91.314
14.83	5.095	1.467	9.412	4.502	54.280	88.272
15.83	5.318	1.502	9.411	4.887	52.470	85.769
20.83	6.748	1.594	9.294	—	46.505	77.834
25.83	8.031	1.622	9.123	—	43.109	73.610
28.83	8.769	1.626	9.020	—	41.638	71.868